American Society of Mechanical Engineers

ASME Accepted Manuscript Repository

Institutional Repository Cover Sheet

Cranfield Collection of E-Research - CERES

ASME Paper Title: Design optimization of supercritical carbon dioxide (s-CO2) cycles for waste heat recovery from marine engines

Authors: Md. J. Hossain, Jahedul Islam Chowdhury, Nazmiye Balta-Ozkan, Faisal Asfand, Syamimi Saadon, Mohammad Imran

ASME Journal Title: Journal of Energy Resources Technology

Volume/Issue: Volume 143, Issue 12 Date of Publication (VOR* Online) 4 March 2021

ASME Digital Collection URL: https://asmedigitalcollection.asme.org/energyresources/article/doi/10.1115/1.4050006/1097038/Design-optimization-of-supercritical-carbon

DOI: https://doi.org/10.1115/1.4050006

*VOR (version of record)

Journal of Energy Resources Technology. Received November 01, 2020;
Accepted manuscript posted January 16, 2021. doi:10.1115/1.4050006
Copyright © 2021 by ASME

Journal of Energy Resources Technology
Volume 143, Issue 12, December 2021 Article number 120901
DOI:10.1115/1.4050006

Design optimisation of supercritical carbon dioxide (s-CO_2) cycles for waste heat recovery from marine engines

Md. Jubayer Hossain
School of Water, Energy and Environment,
Cranfield University, Bedford, MK43 0AL, UK
jubayer.mpe@aust.edu

Jahedul Islam Chowdhury[1]
School of Aerospace, Transport and Manufacturing,
Cranfield University, Bedford, MK43 0AL, UK
j.chowdhury@cranfield.ac.uk

Nazmiye Balta-Ozkan
School of Water, Energy and Environment,
Cranfield University, Bedford, MK43 0AL, UK
n.ozkan@cranfield.ac.uk

Faisal Asfand
School of Computing and Engineering,
University of Huddersfield, Huddersfield, HD1 3DH, UK
F.Asfand@hud.ac.uk

Syamimi Saadon
Department of Aerospace Engineering,
Universiti Putra Malaysia, Selangor, Serdang 43400, Malaysia
mimisaadon@upm.edu.my

Muhammad Imran
Department of Mechanical, Biomedical and Design Engineering,
Aston University, Birmingham, B4 7ET, UK
m.imran12@aston.ac.uk
Member, ASME

[1] Corresponding Author. Email address: j.chowdhury@cranfield.ac.uk (J.I. Chowdhury)

ABSTRACT

The global climate change challenge and the international commitment to reduce carbon emission can be addressed by improving energy conversion efficiency and adopting efficient waste heat recovery technologies. Supercritical carbon dioxide (s-CO_2) cycles that offer a compact footprint and higher cycle efficiency are investigated in this study to utilize the waste heat of the exhaust gas from a marine diesel engine (Wärtsilä-18V50DF, 17.55 MW). Steady-state models of basic, recuperated and reheated s-CO_2 Brayton cycles are developed and optimised for net work and thermal efficiency in Aspen Plus to simulate and compare their performances. Results show that the reheated cycle performs marginally better than the recuperated cycle accounting for the highest optimised net work and thermal efficiency. For the reheated and recuperated cycle, the optimised net work ranges from 648–2860 kW and 628–2852 kW respectively, while optimised thermal efficiency ranges are 15.2–36.3 % and 14.8–35.6 % respectively. Besides, an energy efficiency improvement of 6.3% is achievable when the engine is integrated with an s-CO_2 waste heat recovery system which is operated by flue gas with a temperature of 373 °C and mass flow rate of 28.2 kg/s, compared to the engine without a heat recovery system.

Published by The American Society of Mechanical Engineers. This is the Author Accepted Manuscript issued with: Creative Commons Attribution License (CC BY). The final published version is available online at DOI: 10.1115/1.4050006. Please refer to any applicable publisher terms of use.

1. INTRODUCTION

The temperature of the earth increased by more than 1 °C since 1880 and two-third of the temperature increment has been experienced since 1975 with a rate of approximately 0.15 –0.20 °C per decade [1]. Global warming can cause substantial risks for the climate and humankind including modification of rainfall patterns and the duration of seasons, melting of glaciers, etc. To avoid the adverse effects of climate change, the Paris agreement was signed in 2016 and the long–term temperature goal of this agreement was set to hold the growth of global average temperature less than 2 °C above pre-industrial level with a recommendation to put every effort to limit it within 1.5 °C. This agreement indicated the global emission as the most significant reason for the rise in temperature and suggested to take effective measures to immediately reduce the emissions [2].

Global energy consumption in the form of electricity and heating is nearly 45 % of total energy use [3]. This sector is responsible for the most CO_2 emissions [4] and waste heat [5]. Generation of electricity and heat need a conversion of energy from one form to another. Energy conversion efficiency is one of the major metrics, which can put a considerable limit to rising energy demands, and can also assist in reducing global emission [6]. This is because emission occurs mainly due to conversion losses. Globally, the loss is nearly 72 % with respect to global energy input [3]. The maritime sector has a low profile in the discussions regarding emission and climate change, although it accounts

for around 3 % of the global CO_2 emissions, which is the average value for the period of 2007 to 2012 [7]. Besides, CO_2 emission by international shipping is more than the sixth biggest emitting country, Germany [8]. The International Maritime Organization (IMO) has put efforts into introducing new efficient ships in large numbers, however, these initiatives are not enough to meet the Paris Agreement's climate goal, which indicates that immediate action should be taken to reduce the emission from existing ships [8].

For marine diesel engines, waste heat along with cooling water accounts for taking 50 – 60 % of input fuel energy [9]. Even for low speed marine engines with nearly 50 % efficiency, the exhaust gas constitutes around 50 % of the total waste heat, i.e., 25 % of the fuel energy [10]. When subjected to standard engine design restrictions, this thermal efficiency (nearly 50 %) is very close to the maximum achievable value according to the Carnot theorem [11]. Therefore, it is not possible to improve engine efficiency largely by optimising the traditional in-cylinder thermodynamic cycles. In this context, waste heat recovery (WHR) using thermal power cycles, e.g., Organic Rankine cycle (ORC), steam Rankine cycle (SRC), Trilateral flash cycle (TFC), supercritical carbon dioxide (s-CO_2) cycle, etc., can be an efficient way to generate more power without additional fuel [12–15]. These technologies are usually incorporated as a bottoming cycle in combination with the topping cycle, e.g., the in-cylinder cycle, which considerably improves the combined engine efficiency by generating additional power. This will, consequently, reduce fuel consumption, which, in turn, will facilitate in reducing the emission.

The temperature range of exhaust gas of marine engines is usually considered as 250–600 °C [16]. At this higher temperature, very few bottoming cycles perform efficiently. Conventionally, SRC has the ability to recover heat from such a temperature range. However, due to the space requirement and higher weight, especially comparing to the s-CO_2 cycles, this cycle is not preferred as a bottoming cycle for the ship [17–19]. ORC and similar cycles can be an alternative, but their efficiencies are not reasonably higher at this elevated temperature range. Besides, organic compounds lack thermal stability with the rise of temperature at this range. A suitable alternative is the supercritical carbon dioxide (s-CO_2) cycle, which is suitable for high temperature applications and can operate with higher efficiency in comparison to other bottoming cycles [20].

The s-CO_2 cycle is a closed-loop cycle, where carbon dioxide acts as a working fluid just above its critical point. The CO_2 is compressed at a compressor near its critical point, where the compression work is extremely sensitive to the change in density [21]. Following that, it is heated to a certain temperature in a heater by a suitable waste heat before passing through a turbine and a condenser. This cycle suits mostly with the Brayton cycle. The s-CO_2 has a significantly higher density close to the critical point and shows strong real gas behaviour, which results in high efficiency and enables to downsize of the system components.

Despite its advantages near the critical point, s-CO_2 cycle had not been employed for a long time due to various technological constraints, e.g., complex design of turbomachinery, required lowest and highest cycle-pressure, which are above 74 bar and 260 bar respectively, required pressurization of power plants, etc. These problems could not be addressed appropriately even during the 80s [17]. From the last decade, s-CO_2 cycle has been getting increased attention and in 2011, the Sandia National Laboratories (SNL), USA, declared that they had mastered the necessary technologies required for s-CO_2 cycle [9], which includes the design of compact turbomachinery, constant maintenance of required pressure, etc. Further advancement of this technology makes it suitable to operate as a stand-alone system. However, there are a few researches conducted on WHR of marine engines using s-CO_2 as a bottoming cycle. In fact, in their article published in 2015, Hou et al. [9] mentioned that there was no published research regarding the utilization of waste heat of marine diesel engines with s-CO_2 cycle. Best of the author's knowledge, to this date, there are only a few relevant published literature on s-CO_2, for marine engines [7, 17, 18, 19] although some significant features are completely or partially missing, which include covering the entire range of exhaust gas temperature of marine engine, considering a complete applicable range of maximum cycle-pressure, etc. Besides, no article considers both the net work and thermal efficiency optimisation for sensitivity analysis, which are critical for deciding design parameters for s-CO_2 cycles. There are still a few configurations of the Brayton cycle that need to be

explored further with different system constraints, e.g., reheated Brayton cycle. Hence, the present study represents the performance simulation as well as design optimisation of s-CO_2 cycles, wherein both the net work and the thermal efficiency are optimised separately. The considered temperature range covers almost the entire range of exhaust gas both for the diesel engines and the gas turbines for marine applications. Basic Brayton, recuperated and reheated cycles are simulated, and their performance metrics are analysed and compared to evaluate their potential as a bottoming cycle as well as to assess the merits of thermal integration into the basic cycle.

The remainder of the paper is structured as follows. Section 2 represents a detailed description of the selected thermodynamic cycles. Section 3 depicts the developed methodology required to model and analyse the cycles. Results obtained from each simulation are presented and discussed in section 4. Finally, conclusions are drawn in section 5 along with the scopes of future research.

2. SYSTEMS DESCRIPTION

Based on the engineering constraints and their overall system configurations, the design criteria for s-CO_2 cycle were set to recover the waste heat (WH) from marine engines. The configurations were based on the closed-loop Brayton cycle, wherein s-CO_2 acts as working fluid. The considered system configurations were (a) basic Brayton cycle, (b) Brayton cycle with an internal heat exchanger (recuperator), also known as

recuperated cycle, and (c) Brayton cycle with reheating and recuperation, alternatively known as reheated cycle. The exhaust gas from a marine diesel engine acted as the heating source of the heater for each cycle.

2.1 Basic Brayton Cycle

Fig. 1 represents the basic form of the closed-loop Brayton cycle along with its thermodynamic process in temperature-entropy (T-s) diagram. This is the simplest among all the forms. The operation principle of the Brayton cycle is as follows. A working fluid is passed through the compressor (1–2), wherein its temperature and pressure are increased. The pressurized fluid proceeds into the primary heat exchanger (heater) and in it, heat-addition process takes place by an external source, e.g., the exhaust gas of marine engines (2–3). This results in high temperature fluid, where the pressure is kept ideally constant. This fluid enters and expands into the turbine and produces useful work (3–4). Following that, the fluid passes through another heat exchanger (cooler), wherein a constant-pressure heat rejection process takes place so that the resulting fluid attains the required inlet temperature of the compressor (4–1). This cycle was chosen for further analyses due to its simplest design as well as for the requirements of the minimum number of components. The results obtained from this cycle were also essential to analyse and compare the effect of thermal integration that was incorporated into other cycles.

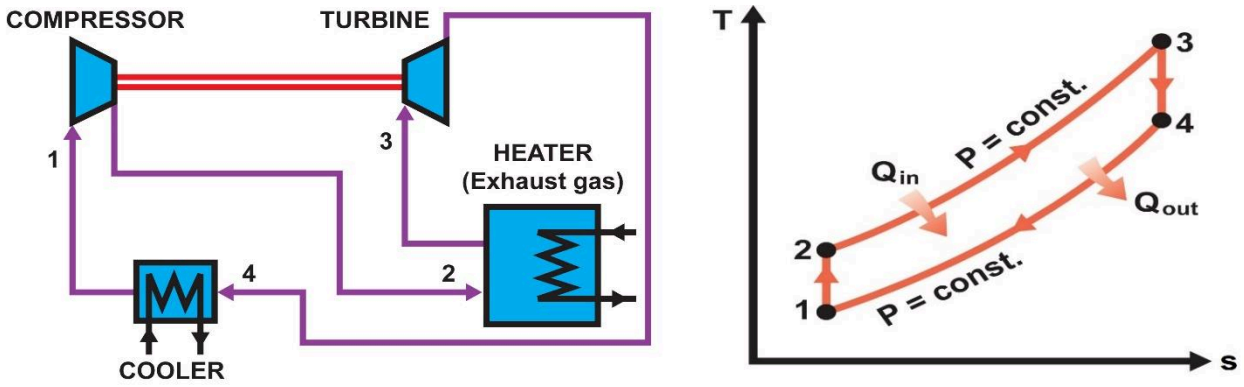

(a) Cycle configuration (b) Thermodynamic process

Fig. 1 Schematic and T-s diagram of the Basic Brayton cycle

2.2 Recuperated Cycle

The recuperated cycle is the integration of an additional counter-flow heat exchanger, known as recuperator or regenerator, to the basic Brayton cycle. Fig. 2 shows the configuration of this cycle that comprises of five major components namely compressor, heater, turbine, recuperator and cooler. This cycle is only used when the temperature of the fluid leaving the turbine is more than the temperature of the fluid leaving the compressor. The working principle is similar to the basic Brayton cycle except that the heat is transferred from the fluid leaving the turbine (5), e.g., hot stream, to the fluid leaving the compressor (2), e.g., cold stream, before heat-addition process starts (3–4). The transfer of heat takes place in the recuperator which, in turn, enhances the overall heat-exchanging performance. This cycle was selected due to the limited design complexity with high recovery of WH and thermal efficiency.

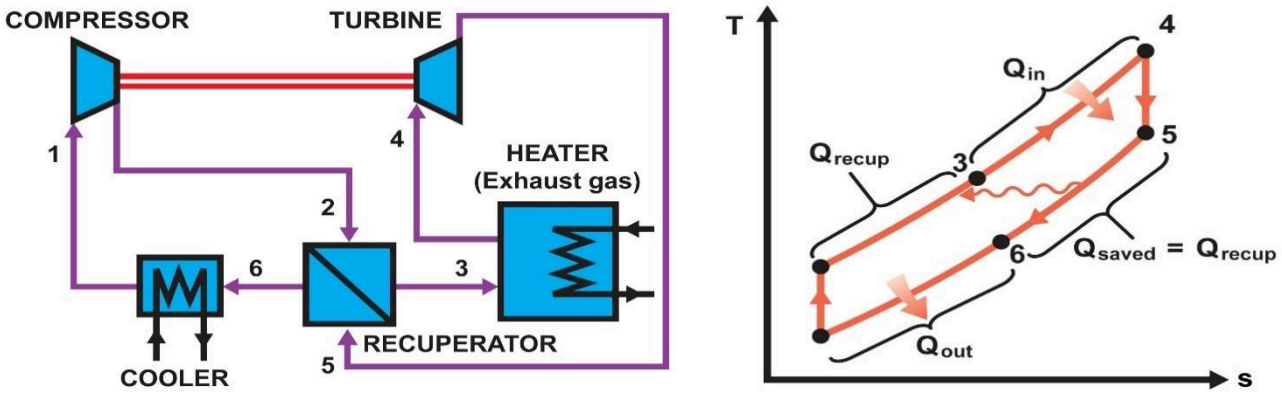

(a) Cycle configuration (b) Thermodynamic process

Fig. 2 Schematic and T-s diagram of the Recuperated cycle

2.3 Reheated Cycle

This is similar to the recuperated cycle except for the expansion process in the turbine, which occurs in two steps. As this cycle is accompanied with recuperation it is also known as the Brayton cycle with reheating and recuperation, or a reheated cycle with recuperation. In this cycle, as can be seen in Fig. 3, the expansion of the fluid is split into two: the fluid exits the heater and passes through the high pressure (HP) turbine (4–5), is heated again through the same heater (5–6), and finally, expands in the low pressure (LP) turbine (6–7).

As the expansion process of the fluid is split into two turbines, it is essential to use the optimum expansion split ratio (ESR), i.e., the pressure ratio (PR) of each turbine at which the cycle will generate maximum power. The expansion split ratio (ESR) can be defined as follows [15]:

Expansion split ratio, $ESR = \frac{PR_{HPT}}{PR_{HPT-ideal}}$ (1)

where, PR_{HPT} is the pressure ratio of the high-pressure turbine and $PR_{HPT-ideal}$ is the pressure ratio of high pressure turbine when the pressure ratio of both turbines are kept equal. When the *ESR* becomes close to one with or without recuperator, the reheated cycle yields maximum specific power [17]. Therefore, the expansion split ratio for the reheated cycle was taken as 1. That means the pressure ratio of both the turbines were assigned with the same value. This layout was selected due to its higher efficiency as well as specific power as a stand-alone cycle.

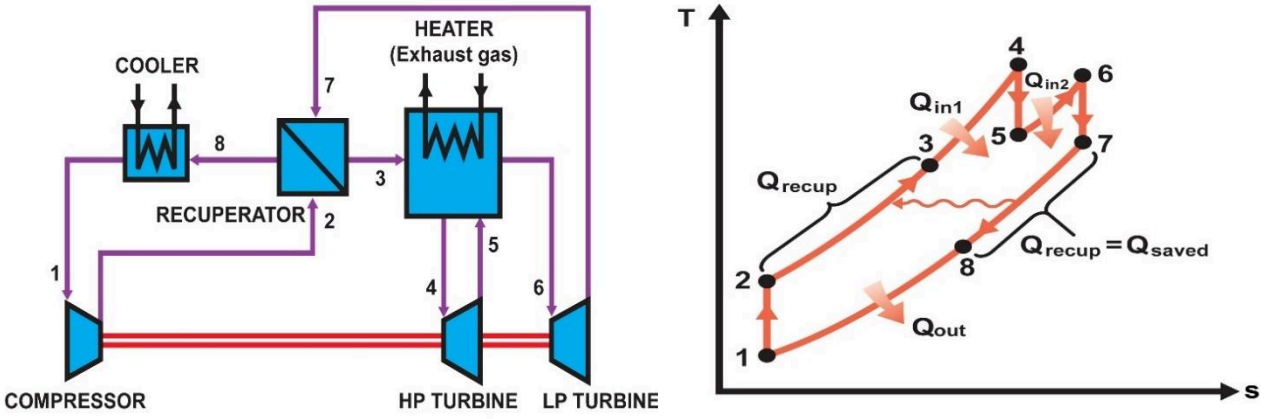

(a) Cycle configuration (b) Thermodynamic process

Fig. 3 Schematic and T-s diagram of the Reheated cycle

3. MODEL DEVELOPMENT

A steady-state modelling approach comprises of a limited but sufficient number of thermodynamic parameters, which can be distinguished easily for system design,

optimisation, and performance evaluation, was considered for all cycles studied in this paper. For each of the components, the governing equations and the complete balance equations, such as mass and energy balance, were framed together. The models were developed on Aspen Plus software, which is widely used to build models for WHR and relevant systems [25,26]. For the present study, Peng-Robinson was chosen for obtaining thermodynamic properties of fluids, which represents accuracy, consistency in critical region and simplicity [27].

3.1 System input parameters and assumptions

As the critical point of s-CO_2 is defined by 31.1 °C and 73.8 bar, the minimum temperature and the pressure of the systems were taken as 32 °C and 75 bar – slightly higher than the critical point to prevent the cycle entering into the transcritical state. These values are within the practically acceptable range [20]. The maximum pressure of the s-CO_2 cycle was considered as 300 bar due to technological constraints, which results in a maximum pressure ratio of 4 [20].

Some simplified standard assumptions were also considered for the selected system configurations, which are as follows:

a) The models were considered as steady-state models with steady-flow conditions.
b) At the inlet and outlet of each component, thermodynamic equilibrium was considered.

c) Approach temperature for heat exchangers is defined as the temperature difference between the outlet temperature of a hot-stream and the inlet temperature of a cold-stream. For all heat exchangers, this temperature was kept at 10 °C.

d) Seawater was considered as a coolant in the cooler. For simplicity, the seawater temperature of 10 °C was assumed.

e) Pressure drops in the systems were not taken into account.

The assumptions regarding turbomachinery were obtained from literature, which are as follows:

a) The compressor isentropic efficiency is 75 % [28].

b) The isentropic efficiency of the turbine is 80 % [29].

3.2 Equations for components

All the components of selected cycle configurations, corresponding to their thermodynamic processes shown in Fig. 1(b), Fig. 2(b), and Fig. 3(b) were modelled using steady state thermodynamic equations.

The steady-state models of different components for basic Brayton, Recuperated and Reheat cycles considered in this research are given as follows [15,30]:

For compressors:

$$T_o = T_i\left(\frac{P_o}{P_i}\right)^{\frac{k-1}{k}} \quad ; \quad k = \frac{C_p}{C_v} \tag{2}$$

$$\dot{W}_C = \dot{m}_{wf}(h_o - h_i) = \dot{m}_{wf}(h_{o-isen} - h_i)/\ \eta_C \quad (3)$$

For heaters:

$$\dot{Q}_{in} = \dot{m}_{wf}\left(h_{wf,o} - h_{wf,i}\right) = \dot{m}_{exh}\left(h_{exh,i} - h_{exh,o}\right) \quad (4)$$

For turbines:

$$T_o = T_i\left(\frac{P_o}{P_i}\right)^{\frac{k-1}{k}} \quad (5)$$

$$\dot{W}_T = \dot{m}_{wf}(h_i - h_o) = \dot{m}_{wf}(h_i - h_{o-isen})\ \eta_T \quad (6)$$

For coolers:

$$\dot{Q}_{out} = \dot{m}_{wf}\left(h_{wf,i} - h_{wf,o}\right) = \dot{m}_w\left(h_{w,o} - h_{w,i}\right) \quad (7)$$

For recuperators:

$$\dot{Q}_{recup} = \dot{m}_{wf}\left(h_{wf,i} - h_{wf,o}\right)_{TS} = \dot{m}_{wf}\left(h_{wf,o} - h_{wf,i}\right)_{CS} \quad (8)$$

where, T_i, T_o and P_i, P_o symbolize the temperature and pressure at the inlet and outlet of a compressor or turbine respectively, $k = \frac{C_p}{C_v}$ is the specific heat ratio, wherein C_p, C_v are the specific heat at constant pressure and constant volume respectively, $\dot{m}_{wf}$ denotes the mass flow rate of s-CO_2, $\dot{m}_{exh}$ represents the mass flow rate of waste heat (exhaust gas), h_i and h_o are the specific enthalpy at the inlet and outlet of a component, h_{o-isen} is the specific enthalpy at compressor or turbine outlet for an isentropic process, η_C and η_T are the isentropic efficiency for compressor and turbine respectively, $\dot{W}_C$ denotes the input work to the compressor and $\dot{W}_T$ symbolizes the output work obtained from the turbine, $\dot{Q}_{in}$ is the total supplied heat energy into the

heater, $\dot{Q}_{out}$ represents the heat rejected into the cooler, and $\dot{Q}_{recup}$ indicates the heat recuperated from turbine exhaust.

3.3 Performance analyses

Typically, thermal efficiency, based on the 1st law of thermodynamics, is utilised to evaluate the performance of thermodynamic cycles. In this study, only the bottoming cycles are taken into consideration, wherein the obtained 'net work' also poses a significant role for the assessment of the cycles. Therefore, both the net work and the thermal efficiency of the cycles were considered to be assessed and compared. The equations that describe the net work and thermal efficiency are as follows [15]:

For basic Brayton and recuperated cycles,

Net work, $\dot{W}_{net,Basic} = \dot{W}_{net,Recup} = \dot{W}_T - \dot{W}_C - \dot{W}_{Cooler}$ (9)

Thermal efficiency, $\eta_{th,Basic} = \eta_{th,recup} = \frac{\dot{W}_{net}}{\dot{Q}_{in-total}} = \frac{\dot{W}_T - \dot{W}_C - \dot{W}_{Cooler}}{\dot{Q}_{in}}$ (10)

For reheated cycle,

Net work, $\dot{W}_{net.Rht} = \dot{W}_{T1} + \dot{W}_{T2} - \dot{W}_C - \dot{W}_{Cooler}$ (11)

Thermal efficiency, $\eta_{th,Rht} = \frac{\dot{W}_{net}}{\dot{Q}_{in-total}} = \frac{\dot{W}_{T1} + \dot{W}_{T2} - \dot{W}_C - \dot{W}_{Cooler}}{\dot{Q}_{in1} + \dot{Q}_{in2}}$ (12)

For all cycles [12],

Heat recovery efficiency, $\eta_{HR} = \frac{\dot{Q}_{in-total}}{\dot{Q}_{ref}} = \frac{\dot{Q}_{in-total}}{\dot{m}_e C_p (T_{e1} - T_{e2})}$ (13)

where, $\dot{Q}_{in-total}$ and $\dot{Q}_{ref}$ are the total recovered heat from waste heat (heat input to the cycle) and maximum recoverable heat respectively, $\dot{m}_e$ is the mass flow rate of

exhaust gas, C_p is the specific heat of exhaust gas at constant pressure, T_{e1} is the maximum temperature of exhaust gas, T_{e2} is the maximum allowable temperature at which the exhaust gas can be released to the environment. Here, T_{e2} is restricted to 110 °C to prevent the acid condensation in the heat exchanger [31].

In this study, 'Mean Absolute Percentage Error (MAPE)' was used for measuring the accuracy of forecasted data. The corresponding equation is as follows [32–34]:

$$MAPE = \frac{1}{n}\sum_{i=1}^{n}\left|\frac{A_i - F_i}{A_i}\right| \times 100 \ \% \tag{14}$$

where, A_i and F_i are the actual and forecasted value respectively, n is the number of points.

3.4 Optimisation

In this study, sensitivity analyses were performed by considering single-objective optimisation, e.g., one objective function was maximised at a time to get the optimum results. Different values of the variable parameters were trialled to obtain the maximum result of each objective function. Two optimising parameters: net work and thermal efficiency, were considered separately. The sensitivity analyses conducted with these parameters were referred to as 'Net Work Optimisation' and 'Thermal Efficiency Optimisation' respectively. The following objective functions [15] were maximised for the variation of mass flow rate of the working fluid, s-CO_2.

3.4.1 Net work optimisation

For basic Brayton and recuperated cycle,

$$Objective\ \ function = \max_{\dot{m}_{wf,min}}^{\dot{m}_{wf,max}} (\dot{W}_T - \dot{W}_C - \dot{W}_{Cooler}) \quad (15)$$

For reheated cycle,

$$Objective\ \ function = \max_{\dot{m}_{wf,min}}^{\dot{m}_{wf,max}} \left(\dot{W}_{T1} + \dot{W}_{T2} - \dot{W}_C - \dot{W}_{Cooler}\right) \quad (16)$$

3.4.2 Thermal efficiency optimisation:

For basic Brayton and recuperated cycle,

$$Objective\ \ function = \max_{\dot{m}_{wf,min}}^{\dot{m}_{wf,max}} \left(\frac{\dot{W}_T - \dot{W}_C - \dot{W}_{Cooler}}{\dot{Q}_{in}}\right) \quad (17)$$

For reheated cycle,

$$Objective\ \ function = \max_{\dot{m}_{wf,min}}^{\dot{m}_{wf,max}} \left(\frac{\dot{W}_{T1} + \dot{W}_{T2} - \dot{W}_C - \dot{W}_{Cooler}}{\dot{Q}_{in1} + \dot{Q}_{in2}}\right) \quad (18)$$

4. RESULTS AND DISCUSSION

The models of the selected s-CO_2 systems were simulated using waste heat data from marine diesel engines (DE). The models were validated first followed by base-case simulations, where both the net work and thermal efficiency were optimised. Finally, sensitivity analyses for each cycle were conducted and the performances of the cycles were analysed.

4.1 Model validation

To validate the software as well as to verify the results obtained from the simulation, basic Brayton cycle was modelled and simulated to reproduce the results which was used to compare the data from existing literature. Hou et al. [9] performed a simulation for the closed-loop basic Brayton cycle using Aspen plus software, wherein the thermodynamic properties of CO_2 were calculated using the NIST REFPROP property method. In their study, the exhaust gas of a marine diesel engine was considered as the waste heat source. The major input parameters for both studies are summarised in Table 1 and for those inputs, the obtained results are compared and shown in Fig. 4.

The trend of the curve as well as the results obtained from the simulation of present study are of a good match with the study of Hou et al. [9]. The mean absolute percentage error (MAPE), which is a measure of prediction accuracy of a forecasting method in statistics, was calculated as 4.45 % approximately. This small deviation is due to the different approaches that were used for calculating the thermodynamic properties of fluids. In this study, Peng-Robinson property method was used, whereas NIST REFPROP was employed for the reference study.

Table 1 Input parameters for validation

Input parameters	**Value (Unit)**
Compressor inlet temperature	31 (°C)
Compressor inlet pressure	74 (bar)
Compressor outlet pressure range	130–200 (bar)
Heater inlet temperature (exhaust gas)	290 (°C)

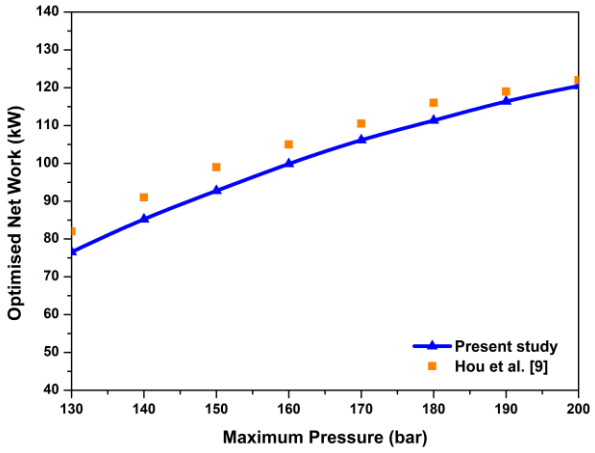

Fig. 4 Validation of current model with respect to variation of optimised net work output with maximum pressure

4.2 Base-case results

The system configuration with aptly defined input parameters, on which all the simulations and analyses were performed, is termed here as a base-case. The exhaust gas temperature range of marine DE is usually considered as 250–600 ^{o}C, although the range

becomes a bit lower if the engine comes with a turbocharger. This temperature range also covers the entire range (370–540 ^{o}C) of marine gas turbines [16]. Apart from its advantage regarding high temperature, the waste heat recovery (WHR) process from DE is preferred as the WH energy, which is approximately 25-30% of the total energy supplied through fuel [16]. Therefore, a diesel engine is considered for the base-case. Among various types of DE, Wärtsilä-18V50DF model [35] was selected for base-case analysis. This engine produces 17.55 MW power with an engine efficiency of 47 % and the exhaust gas after turbocharging remains at 373 °C with a mass flow rate of 28.2 kg/s [36]. All the required major data for this base-case study are summarised in Table 2. With these input parameters, required optimisation points were achieved by varying the flow rate of s-CO2 from 1.5–40 kg/s with an increment of 0.5 kg/s. For each mass flow rate, net work and thermal efficiency were obtained.

Table 2 Base-case parameters for marine diesel engine

Components	Parameters	Value (unit)	Source
Compressor	Inlet temperature	32 (°C)	[20]
	Inlet pressure	75 (bar)	[20]
	Pressure ratio	4	[20]
	Isentropic efficiency	75 (%)	[28]
Heater (Hot stream / waste heat)	WH temperature	373 (°C)	[36]
	WH mass flow rate	28.2 (kg/s)	[36]
	Approach temperature	10 (°C)	[40]
Turbine	Expansion ratio	4[a]	[20]
	Isentropic efficiency	80 (%)	[29]
Cooler (Cold stream / sea water)	Water temperature	10 (°C)	Assumption
	Approach temperature	10 (°C)	[40]

[a] For the basic Brayton and Recuperated cycles, the expansion ratios were 4. The expansion ratio of each of the two turbines in the reheated cycle were kept equal to 2.

For the basic Brayton cycle, the obtained results are shown in Fig. 5. It can be seen from the figure that for the increase of mass flow up-to 19.5 kg/s, the net work rises

linearly and reaches its peak (1000.96 kW) before falling gradually. Therefore, 1000.96 kW was regarded as optimised net work, which was achieved at s-CO_2 mass flow rate of 19.5 kg/s. Thermal efficiency, although remains almost constant (14.17 %) up to the flow rate of 19 kg/s, falls gradually with a further increase of mass flow rate. Hence, 14.17 % was taken as optimised thermal efficiency, wherein the flow rate was considered as 19 kg/s.

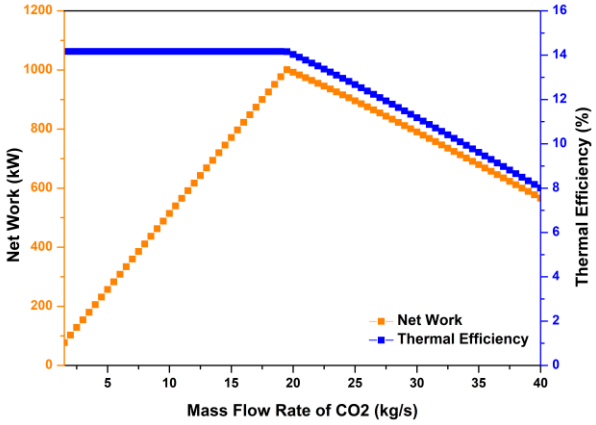

Fig. 5 Determination of optimised mass flow rate of CO_2 for basic Brayton cycle from the waste heat data of diesel engine

Similarly, the optimum net works for the recuperated and reheated cycles were found at s-CO_2 flow rates of 21.5 kg/s and 20.5 kg/s respectively, while for the thermal efficiency optimisation they were 21 and 20 kg/s respectively. The computed results for each cycle are summarised in Table 3. It is evident that the reheated cycle yields both the maximum net work (1107.21 kW) and thermal efficiency (22.4 %). However, basic Brayton cycle performed well in terms of heat recovery, which accounts for the highest heat recovery efficiency, i.e., 89.91 % due to the absence of a recuperator or regenerator.

Recuperator preheats the working fluid leaving the compressor and makes it comparatively hotter before entering the heater. Therefore, the preheated working fluid recovers less heat from the main heater to attain the same turbine inlet temperature comparing to non-preheated fluid within the same system conditions. Basic Brayton cycle does not feature a recuperator; thus, recovers more heat comparing to the cycles with a recuperator. As the heat recovery efficiency is the ratio of the actual recovered heat to the maximum recoverable heat basic cycle poses the highest heat recovery efficiency. However, for such cycles, required cooling work in the cooler becomes more due to the increased temperature of the incoming hot stream, which, in turn, reduces the net work as well as thermal efficiency. Due to the increased cooling work and absence of recuperation, basic Brayton cycle generates the least net work and thermal efficiency despite being the highest heat-recovered cycle.

Table 3 Base-case results for marine diesel engine

Parameters	Basic Brayton cycle		Recuperated cycle		Reheated cycle	
	Optimised $\dot{W}_{net}$	Optimised η_{th}	Optimised $\dot{W}_{net}$	Optimised η_{th}	Optimised $\dot{W}_{net}$	Optimised η_{th}
Turbine work (kW)	2204.87	2150.03	2413.62	2376.35	2365.51	2316.10
Compressor work (kW)	1186.2	1155.78	1304.82	1277.44	1247.03	1216.61
Pump work for cooling (kW)	17.71	17.28	11.83	11.56	11.27	11.00
Heat input (kW)	7068.45	6896.02	5143.05	5046.44	4970.78	4859.78
Net work (kW)	1000.96	976.98	1094.00	1087.35	1107.21	1088.49
Thermal efficiency (%)	14.16	14.17	21.31	21.55	22.27	22.40
Heat recovery efficiency (%)	89.91	87.72	65.42	64.19	63.23	61.82
Engine efficiency without WHR (%)	47	47	47	47	47	47
Engine efficiency with WHR (%)	49.68	49.62	49.93	49.91	49.97	49.92

4.3 Sensitivity analyses

Sensitivity analyses are performed to observe the system behaviour, when some parameters are varied from their optimised system-conditions. In this study, two parameters: waste heat temperature and maximum pressure were varied. It is worth noting that the sensitivity for waste heat mass flow rate variation is not included due to the fact that system performance such as thermal efficiency is unaffected with the variation of waste heat flow rate. For the variation of independent variables (temperature of flue gas and pressure of the cycle), all the selected cycles were optimised separately for both the net work and the thermal efficiency. The summary of inputs used for optimisation is shown in Fig. 6.

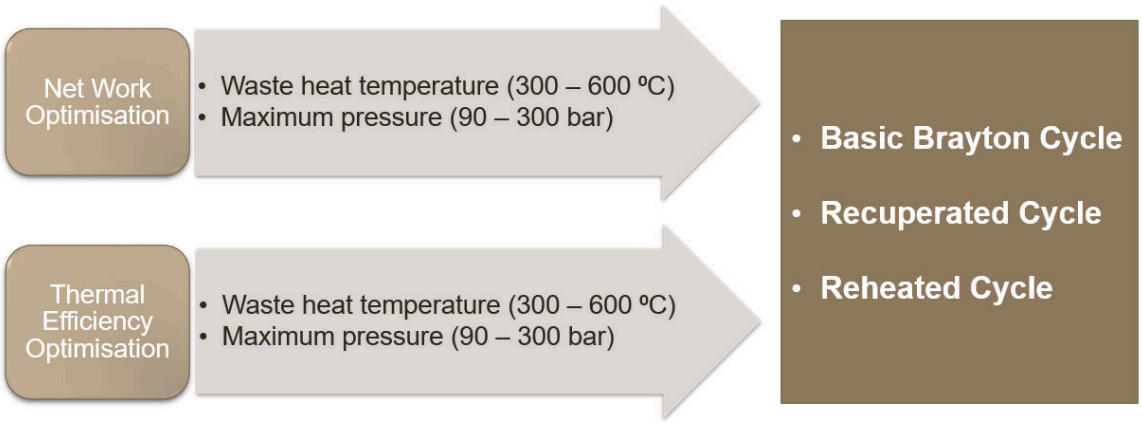

Fig. 6 Summary of input parameters for sensitivity analysis

4.3.1 Waste heat temperature variation

The waste heat temperature (WHT) was varied widely from 300–600 °C with an increment of 20 °C, covering almost all the range of exhaust gas temperature of marine diesel engines and gas turbines. Both the net work and thermal efficiency were optimised in separate analyses and corresponding parameters were obtained. These optimised results are presented in Fig. 7 and Fig. 8 respectively.

With the increase of waste heat inlet temperature, the optimised net work rises gradually for each cycle as shown in Fig. 7(a). This is due to the fact that the net work is a function of mass flow rate of working fluid and the specific enthalpy of turbine, i.e., turbine inlet temperature. As WHT rises, turbine inlet temperature also increases. Thus, the specific enthalpy increases at turbine inlet and consequently, generates more work after the expansion. This finding matches with the studies conducted by Chowdhury et al. [31] and Hou et al. [9], although their considered temperature ranges were somewhat lower than the current study.

Fig. 7(a) also shows that both the recuperated and reheated cycles generate more work than that of basic cycle. This is due to the presence of a recuperator in both cycles, which facilitates to preheat the working fluid (s-CO_2) leaving the compressor before entering the heater. Due to this temperature increment, s-CO_2 requires less heat from the heater to attain the maximum turbine inlet temperature and the rest of the available heat is used to increase the mass flow rate of s-CO_2. With the increase of s-CO_2 flow rate and

turbine inlet temperature, a higher net work for the recuperated and reheated cycles can be obtained. This outcome is of a good match with the results obtained by Hou et al. [9], where they concluded that recuperated cycle produced considerably more net work than basic cycle. Although the curves of the recuperated and reheated cycle tend to overlap, reheated cycle performs marginally better. The net work produced by reheated cycle is in the range of 648.08–2860 kW, while recuperated cycle yields 628.13–2852.68 kW. The highest net work (2860 kW) is achieved at the highest WHT (600 °C) by reheated cycle.

Fig. 7 (b) depicts the change in thermal efficiency corresponding to optimised net work value. The trend is similar to the net work. Besides, reheated and recuperated cycle performed much better than the basic Brayton cycle due to the incorporation of recuperator in their cycle configurations. This fact is discussed comprehensively with results from the thermal efficiency optimisation in a the later section. Although reheated and recuperated cycles represent adjacent curves, thermal efficiency of the reheated cycle is slightly higher than the recuperated cycle at all points. The range is 15.60–29.08 % and the maximum efficiency occurs at 600 °C – the same temperature at which maximum net work was attained.

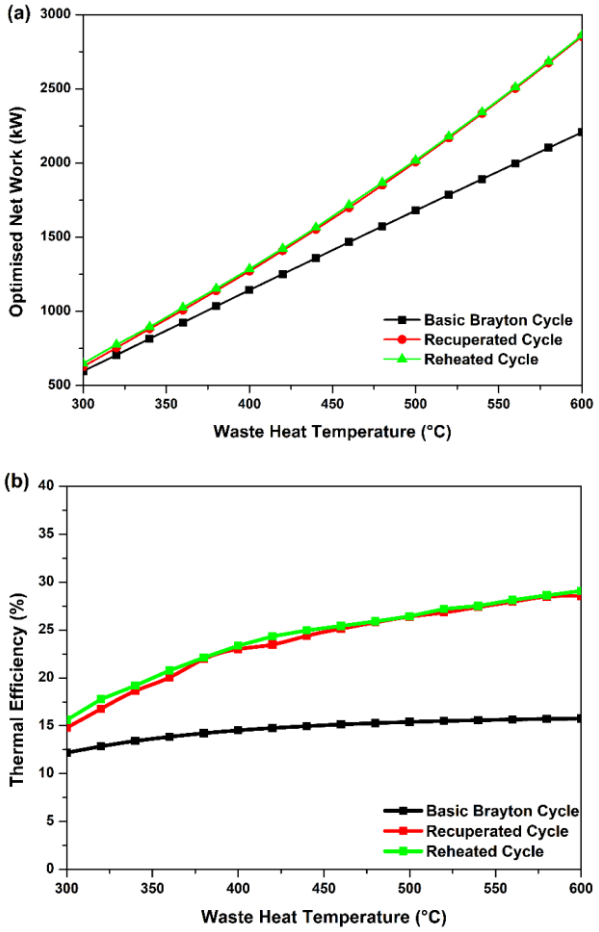

Fig. 7 Effect of variation of waste heat inlet temperature for (a) optimised net work and (b) corresponding thermal efficiency

Similar analyses like the net work optimisation in Fig. 7(a) had been conducted by optimising the thermal efficiency. The results are shown in Fig. 8. It can be seen from Fig. 8(a) that there is a significant change in optimised thermal efficiency with respect to WHT. Thermal efficiency is primarily a function of turbine inlet temperature and this temperature mostly depends on WHT. With the rise of WHT, each cycle tends to maximise turbine inlet temperature, which, in turn, increases the enthalpy across the turbine, i.e.,

turbine work. This increment of turbine work becomes more than the corresponding additional heat input that occurred due to the increase of WHT. This causes the - thermal efficiency to be increased for all cycles. However, reheated and recuperated cycles performed much better than the basic Brayton cycle. This is due to the incorporation of a recuperator or regenerator in their cycle configurations. As the basic cycle does not feature the recuperator, it cannot preheat the working fluid before entering the heater and hence, requires comparatively more heat input to reach the same turbine inlet temperature. Since thermal efficiency is the ratio of net work to heat input, thermal efficiency obtained by the basic cycle is comparatively lower. This is also the case for the study conducted by Hou et al. [9].

Thermal efficiency yield by reheated cycle is higher than recuperated cycle at all points. The range is 15.20–36.3 % for reheated cycle, where maximum efficiency occurs at 600 °C. Interestingly, this maximum value of thermal efficiency (36.3 %) is higher compared to the corresponding maximum efficiency (29.08 %) obtained while net work optimisation – denoting nearly 24.83 % increment in thermal efficiency optimisation.

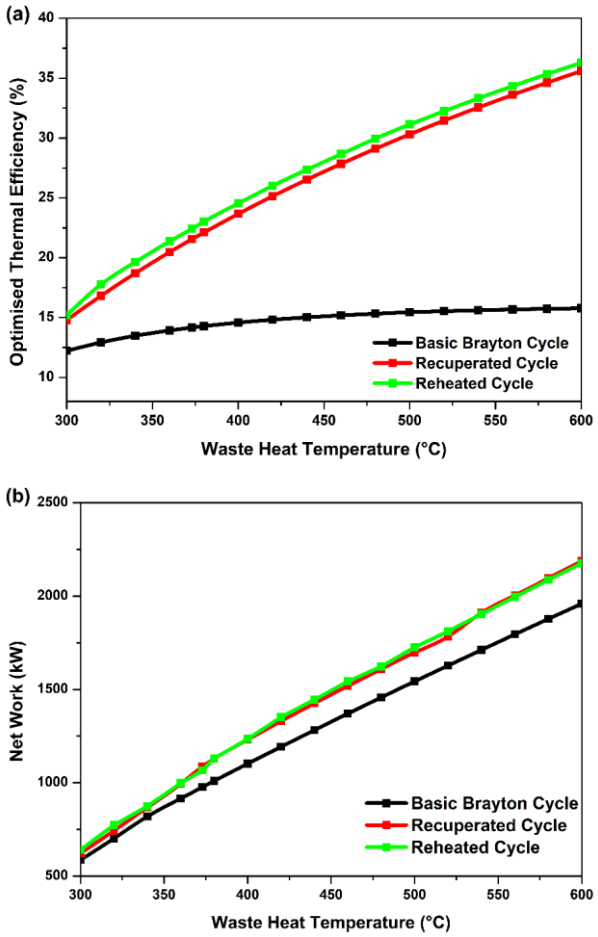

Fig. 8 Effect of variation of waste heat inlet temperature for (a) optimised thermal efficiency and (b) corresponding net work

The change in net work corresponding to the optimised thermal efficiency value is presented in Fig. 8(b). Similar to the net work optimisation, the net work curves represent the identical trend – all the cycles observe increased net work with WHT. Basic cycle accounts for the least net work, whereas reheated cycle produces the highest work almost in all points. The maximum net work (2188.22 kW) is observed at a maximum value of WHT (600 °C). Like the thermal efficiency, a similar contrasting effect is observed for net work. The highest net work (2188.22 kW) obtained by the thermal efficiency

optimisation is considerably lower than the maximum net work generated (2860 kW) while net work optimisation, which implies nearly 30.7 % increment for net work optimisation. These contrasting features both for the net work and the thermal efficiency optimisation are discussed further in section 4.4.

4.3.2 Maximum pressure variation

In this study, the maximum pressure was achieved at the outlet of the compressor and considered constant before the expansion stage. This pressure was varied up to 300 bar– the current maximum applicable limit [20]. For this variation, net work and thermal efficiency were optimised and obtained results are presented in Fig. 9 and Fig. 10 respectively.

Both the optimised net work and corresponding thermal efficiency rise with the increase of maximum pressure for all cycles (Fig. 9). For each case, the reheated cycle generates more output followed by the recuperated and basic cycles, although the rate of increment for net work and thermal efficiency gradually diminishes with the increase of maximum pressure and after 220 bar, the curves become plateaued for reheated and recuperated cycles. Net work is mainly the difference between turbine work and compressor work, both of which depend on the enthalpy difference between their inlet and outlet. With the increase of maximum pressure, the enthalpy difference increases for both components, although the rate of increment is more for turbine. This gives a rise in net work initially. As the rate of increment of turbine work lowers gradually due to the

nature of the property curves, i.e., entropy, temperature lines, the increase in net work diminishes as well. After 220 bar, the increment rate becomes nearly insignificant for reheated and recuperated cycles. This results in almost the same net work with a further increment of maximum pressure. Similar scenario is observed for thermal efficiency as it depends on the net work. The ranges of generated net work and thermal efficiency for the reheated cycle are 573.62–1126.09 kW and 13.68–21.62 % respectively. These findings are a good match with the result obtained by Hou et al. [9]. Their obtained curves for net work and thermal efficiency plateaued after 220 bar for reheated cycle that is the same as the present study.

Fig. 10 represents the results obtained by thermal efficiency optimisation. With the maximum pressure, both the optimised thermal efficiency and corresponding net work increase except a few points. The reheated and recuperated cycle perform better than the basic cycle and their curves start plateauing after 220 bar due to the same reason discussed at net work optimisation.

Reheated cycle accounts for the highest optimised efficiency and corresponding net work for all points. The values of maximum thermal efficiency and net work were observed as 23.8 % and 1105.65 kW respectively, whereas those were 21.62 % and 1126.09 kW respectively for the net work optimisation – again denoting the contrasting effect between two types of optimisation. Although both the net work and thermal efficiency increases with maximum pressure up to a considerable limit, before selecting

the highest operating maximum pressure, associated costs and benefits should be considered at the same time because higher pressure causes substantial costs and extra precautions to manipulate [9].

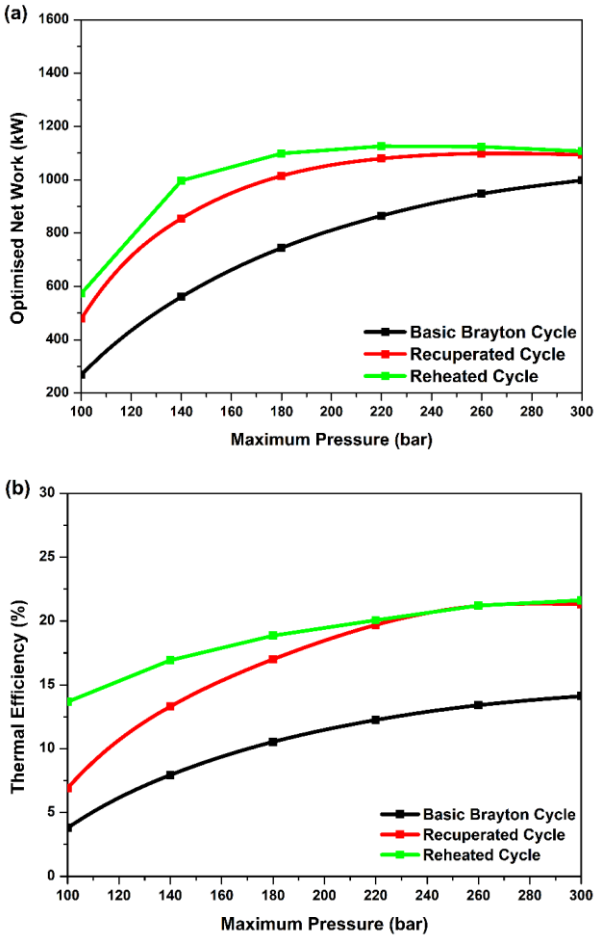

Fig. 9. Effect of variation of maximum pressure for (a) optimised net work and (b) corresponding thermal efficiency

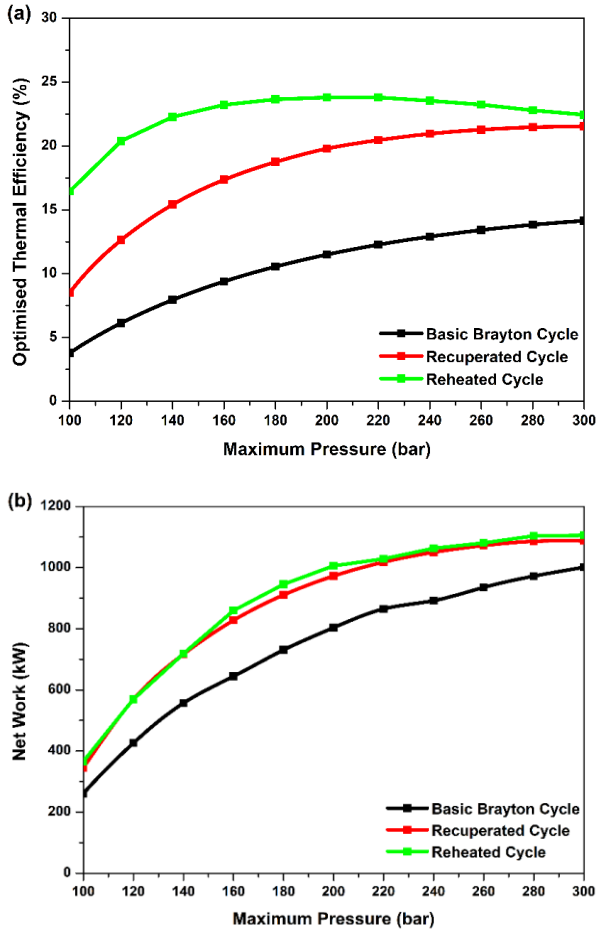

Fig. 10 Effect of variation of maximum pressure for (a) optimised thermal efficiency and (b) corresponding net work

4.3.3 Summary of sensitivity analysis

Considering both types of optimisation, it is observed that reheated cycle performed better than recuperated cycle. As a stand-alone cycle, reheated cycle is more efficient and generates more specific power than that of recuperated cycle [17] – presenting a good fit with the current study. However, in the present study, only bottoming cycles were considered. Brighenti [17] compared reheated and recuperated

cycle for s-CO_2 as bottoming cycles and concluded that recuperated cycle performed better than reheated cycle – which is in disagreement when the cycles are used as a stand-alone system as well as with the present study. However, Brighenti also mentioned that turbine inlet temperature for both the turbines of reheated cycle were kept the same in that study, which imposed additional constrain to the system and might reduce the overall flexibility of the optimisation process.

Although net work is a function of both turbine inlet temperature and the mass flow rate of working fluid, the influence of the mass flow rate is more. When both the turbine inlet temperatures are maintained the same in the reheated cycle, the mass flow rate of s-CO_2 becomes eventually lower due to the fixed heat input of the bottoming cycles. This reduced mass flow results in comparatively reduced net work and thermal efficiency. Thus, the performance of reheated cycle becomes poorer than recuperated cycle – the conclusion deduced by Brighenti [17]. In the present study, the turbine inlet temperatures were not set as the same in reheated cycle, which ensured the enhanced flexibility in the optimisation process. Therefore, both the turbine inlet temperature as well as the mass flow rate were sufficiently maximised in all analyses, which resulted in maximum possible net work and highest thermal efficiency for reheated cycle. Therefore, it can be concluded that reheated cycle performed best among all cycles for the variation of WHT and maximum pressure.

At a similar temperature range (300–550 °C), the comparable technology like ORC yields only 16–17 % net efficiency [37], which indicates a good increment in efficiency for the s-CO_2 cycles. Besides, at this temperature range, most of the organic fluid lacks sufficient thermal stability. The steam Rankine technology, operated at this temperature range, has also experienced lower efficiency than s-CO_2 cycles [20] and the space requirements are also higher than that of s-CO_2 cycles. Persichilli et al. [38] compared steam Rankine cycle (SRC) with the s-CO_2 cycle for recovering WH from a stationary gas turbine. The study denoted that s-CO_2 cycle generated more power than the single-pressure SRC and was comparable with dual-pressure SRC. Besides, the space requirement for installing this s-CO_2 cycle was less than nearly two-third of the SRC, which indicates lower installation cost with a quicker start-up.

Apart from generating large useful work, this sensitivity analysis also depicts another significant observation. At the maximum net work point, the outlet temperature of the waste heat becomes 275 °C. This denotes that if this cycle is introduced as a bottoming cycle, the exhaust gas temperature of the marine engine will decrease to 275 °C from 600 °C – a 54.17 % drop from its initial value. At this operating point, heat recovery efficiency reaches 67.16 % – a significant amount to consider. These will, consequently, contribute to reducing thermal pollution as well as the increment rate of global warming.

4.4 Optimised net work or optimised thermal efficiency?

Interestingly, the highest net work values obtained from net work optimisation and thermal efficiency optimisation are not the same. For the variation of WHT, the highest net work obtained in net work optimisation is 2860 kW (Fig. 7 (a)), whereas the value is 2188.22 kW for thermal efficiency optimisation (Fig. 8 (b)), which denotes nearly 30.7 % increment while net work optimisation. Similar contrasting effect is observed for thermal efficiency which can be compared from Fig. 7(b) and Fig. 8(a) respectively. With the rise of WHT, the maximum thermal efficiency is observed as 29.08 % for net work optimisation, while thermal efficiency optimisation yields 36.3 %. This clearly shows an increment of nearly 24.83 % for thermal efficiency optimisation.

Net work is essentially a function of mass flow rate of working fluid and turbine inlet temperature. However, the influence of mass flow rate is considerably more than the turbine inlet temperature. While net work optimisation is performed, with increased WHT, the cycles try to increase the mass flow rate as much as possible to ensure the generation of maximum net work. Here, the system focuses more on s-CO_2 flow rate than turbine inlet temperature and generates maximum achievable net work within system input. Therefore, the maximum net work obtained by net work optimisation becomes more than the maximum net work yielded by thermal efficiency optimisation. However, this is not the case for thermal efficiency optimisation. Thermal efficiency is mostly a function of turbine inlet temperature and not a function of mass flow rate of working fluid.

Therefore, while the thermal efficiency optimisation is conducted, with the increase of WHT, the system tends to attain the highest turbine inlet temperature to maximise the thermal efficiency regardless of s-CO_2 flow rate. The system emphasises maximising the turbine inlet temperature and the produced thermal efficiency becomes the maximum attainable thermal efficiency. Therefore, maximum efficiency obtained from the thermal efficiency optimisation is more than that of the net work optimisation. These opposing effects were also observed in the simulation of base-cases and maximum pressure variation in the cycles. The study conducted by [39] also produced similar contrasting results for gas turbines. They performed sensitivity analyses by optimising both the net work and thermal efficiency for basic, reheated, intercooled cycle, where each cycle yields opposing effects for the variation of maximum pressure.

Between net work and thermal efficiency, net work is considered as the most important parameter for the present study. This is the useful work recovered from exhaust gas, which does not incur additional fuel consumption. Therefore, obtaining the highest net work is considered as the primary parameter for analysing the systems. Thermal efficiency, which is the ratio of net work output to heat input, is usually the most important parameter for a stand-alone system, where the amount of heat input is of utmost importance as it is related to the fuel consumption, i.e., fuel cost. However, the present study considers only the bottoming cycles, where input heat is extracted from the exhaust gas that costs nothing – causing the thermal efficiency as the secondary

parameter. Therefore, while choosing the optimum design point, the point with the highest net work should be given more priority.

4.5 Engine performance improvement

In this study, a 17.55 MW diesel engine, with exhaust gas temperature of 373 °C and mass flow rate of 28.2 kg/s, was selected. The engine comes without a WHR system and denotes an engine efficiency of 47 %. After WHR with the selected bottoming s-CO_2 cycles, the combined work output and efficiency increased for all cycles. These are shown in Fig. 11. Fig. 11(a) shows the net work obtained before and after deploying WHR cycles. Before WHR, the net work was 17550 kW and after WHR, the combined net work reached as high as 18657 kW for reheated cycle, where each bottoming cycle produced more than 1000 kW. This additional useful power comes from the exhaust gas, which does not incur additional fuel cost. New engine efficiencies, attained after WHR, are presented in Fig. 11 (b). The maximum efficiency was obtained as 49.97 % for reheated cycle, which denotes a 6.3 % improvement in engine efficiency. These improvements will result in less fuel supply requirement, which, in turn, will facilitate reducing CO_2 emission. Besides, the final temperature of exhaust gas at this operating condition reduced from 373 °C to 203.17 °C. This caused a considerable heat recovery efficiency of 63.23 %, which, consequently, would contribute considerably to reduce thermal pollution. If the studied engine is being operated with higher exhaust gas temperature or flow rate, the efficiency would become even more. For instance, when the temperature is raised to 600 °C instead of 373 °C, the

increase in efficiency will be as high as 16.3 % for reheated cycle and when the flow rate of exhaust gas is increased up to 45 kg/s instead of 28.2 kg/s, the efficiency increment will be of 10.04 %.

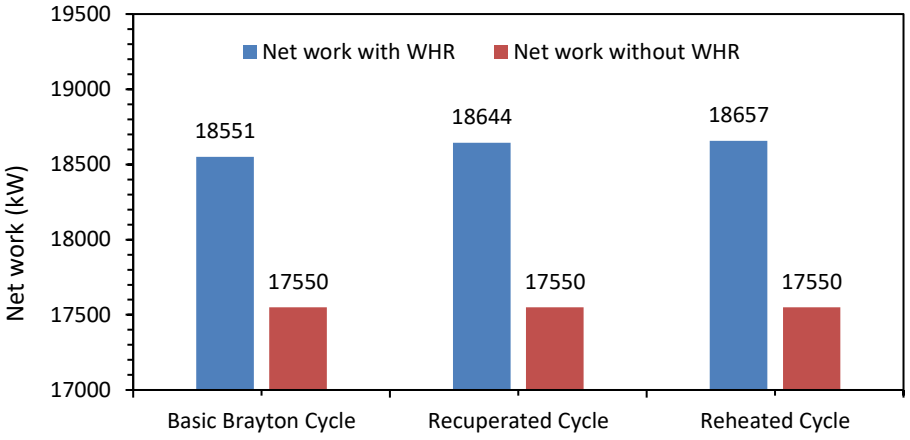

(a) Net work with and without waste heat recovery

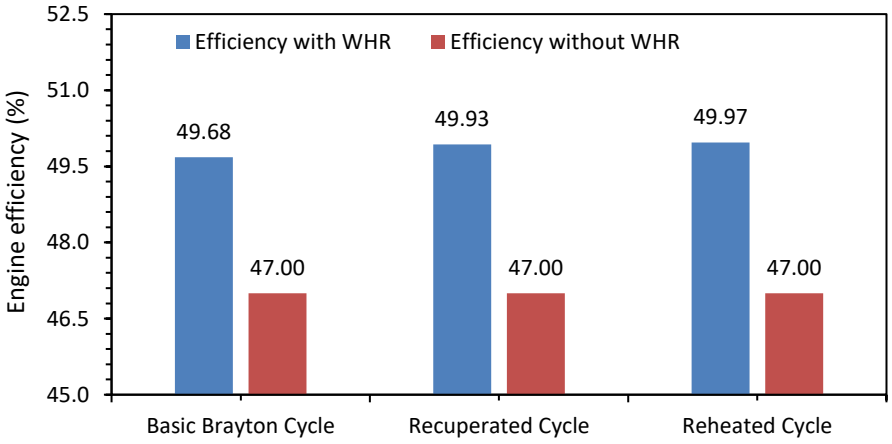

(b) Engine efficiency with and without waste heat recovery

Fig. 11 Engine (Wärtsilä-18V50DF) efficiency improvement with WHR for base-case simulation

5. CONCLUSIONS

In this study, waste heat recovery from the exhaust gas of marine engines using s-CO_2 cycles was investigated. Three closed-loop Brayton cycle configurations (basic Brayton, recuperated, and reheated cycles) were studied to evaluate the performances of s-CO_2 cycles in recuperating the waste heat in marine engines. Basic cycle was selected due to its simplest design as well as for the minimal number of component requirements. Recuperated cycle was chosen because of limited complexity with high recovery of waste heat while the reheated layout was selected due to its higher efficiency and specific power output as a stand-alone cycle. This study represents the performance simulation as well as design point optimisation of selected cycles in terms of waste heat to power production.

Results for the base case of a marine diesel engine considering all the selected s-CO_2 cycles showed that the efficiency of the diesel engine can increase to 49.97 % from 47 % – a well desired 6.3 % increment in engine efficiency indicating a considerable range of waste heat recovery. Sensitivity analyses were conducted by varying input parameters and performing a single objective optimisation, where net-work and thermal efficiency were optimised separately to evaluate the design performance of each cycle. For each type of optimisation, reheated and recuperated cycles produced more net-work and also thermal efficiency than that of basic Brayton cycle. Reheated cycle performed marginally better than recuperated cycle and accounted for the highest generation of net-work and thermal efficiency.

Although the reheated cycle yields the highest net-work and thermal efficiency, the performance of the recuperated cycle was very close to reheated cycle. Unlike recuperated cycle, the reheated cycle requires additional turbine for its two-stage expansion process, which may incur additional cost and space. Therefore, to choose the most feasible configuration between the two, further analyses are needed in terms of cost and space requirements depending on the intended application. Besides, the basic Brayton cycle can also be deployed for the exhaust gas of comparatively lower temperature, for which generated recuperation effect is negligible.

ACKNOWLEDGMENT

None.

FUNDING

No funding to declare.

NOMENCLATURE

Abbreviations

DE	Diesel Engine
ESR	Expansion Split Ratio
GISS	Goddard Institute for Space Studies
HP	High Pressure

IMO	International Maritime Organization
LP	Low Pressure
MAPE	Mean Absolute Percentage Error
NASA	National Aeronautics and Space Administration
NIST	National Institute of Standards and Technology
ORC	Organic Rankine Cycle
PR	Pressure Ratio
s-CO_2	Supercritical Carbon Dioxide
SNL	Sandia National Laboratories
SRC	Steam Rankine Cycle
TFC	Trilateral flash cycle
WH	Waste Heat
WHR	Waste Heat Recovery
WHT	Waste Heat Temperature

Symbols

A	actual value
C	specific heat, J/kg °C
F	forecasted value

h	specific enthalpy, J/kg
K	specific heat ratio
n	no of points
P	pressure (bar)
s	specific entropy
T	Temperature, ° C
$\dot{m}$	mass flow rate, kg/s
$\dot{Q}$	heat transfer rate, kW
$\dot{W}$	Work, kW

Greek letters

η	Efficiency, %

Subscripts

isen	isentropic
wf	working fluid
v	Volume
C	compressor
T	Turbine
th	Thermal

in	in/inlet
out	out/outlet
recup	recuperator
net	net work
Rht	Reheated
HR	heat recovery
ref	reference
e	exhaust gas
min	minimum
max	Maximum
HPT	high pressure turbine

REFERENCES

1. Lenssen NJL., Schmidt GA., Hansen JE., Menne MJ., Persin A., Ruedy R., et al. Improvements in the GISTEMP Uncertainty Model. Journal of Geophysical Research: Atmospheres. 2019; 124(12): 6307–6326. Available at: DOI:10.1029/2018JD029522
2. United Nations Framework Convention on Climate Change. The Paris agreement. 2020.
3. Forman C., Muritala IK., Pardemann R., Meyer B. Estimating the global waste heat potential. Renewable and Sustainable Energy Reviews. Elsevier; 2016; 57: 1568–1579. Available at: DOI:10.1016/j.rser.2015.12.192
4. Wong KV. Sustainable Engineering in the Global Energy Sector. Journal of Energy Resources Technology, Transactions of the ASME. 2016; 138(2): 1–4. Available at: DOI:10.1115/1.4031783
5. Wong K V., Dai Y., Paul B. Anthropogenic Heat Release Into the Environment. Journal of Energy Resources Technology. 2012; 134(4): 1–5. Available at: DOI:10.1115/1.4007360
6. Eichhammer W., Fleiter T., Schlomann B., Faberi S., Fioretto M., Piccioni N., et al. Study on the Energy Savings Potentials in EU Member States, Candidate Countries and EEA Countries. Grenoble; 2009.
7. Smith TWP., Jalkanen JP., Anderson BA., Corbett JJ., Faber J., Hanayama S., et al. Third IMO Greenhouse Gas Study 2014. Third IMO GHG study 2014. London; 2015. Available at: DOI:10.1007/s10584-013-0912-3
8. UK Energy Research Centre. Efficient new ships won't be enough to meet the Paris Agreement's goals. 2020.
9. Hou S., Zhang W., Zeng Z., Ji J. Supercritical CO2 Cycle System Optimization of Marine Diesel Engine Waste Heat Recovery. International Conference on Advances in Energy, Environment and Chemical Engineering. Atlantis Press; 2015. pp. 178–183. Available at: DOI:10.2991/aeece-15.2015.36
10. Zhu S., Zhang K., Deng K. A review of waste heat recovery from the marine engine with highly efficient bottoming power cycles. Renewable and Sustainable Energy Reviews. March 2020; 120: 109611. Available at: DOI:10.1016/j.rser.2019.109611
11. MAN Diesel&Turbo. How to influence CO2. 2014.
12. Chowdhury JI., Nguyen BK., Thornhill D. Investigation of waste heat recovery system at supercritical conditions with vehicle drive cycles. Journal of Mechanical Science and Technology. 2017; 31(2): 923–936. Available at: DOI:10.1007/s12206-017-0145-x
13. Chowdhury JI. Modelling and Control of Waste Heat Recovery System. Queens University Belfast; 2017. Available at: https://ethos.bl.uk/OrderDetails.do;jsessionid=E3C1932C1B35024C5154493AC86

5CC3E?uin=uk.bl.ethos.725593

14. Chowdhury JI., Nguyen BK., Thornhill D., Hu Y., Soulatiantork P., Balta-Ozkan N., et al. Fuzzy Nonlinear Dynamic Evaporator Model in Supercritical Organic Rankine Cycle Waste Heat Recovery Systems. Energies. 2018; 11(4): 901. Available at: DOI:10.3390/en11040901
15. Ajimotokan HA., Sher I. Thermodynamic performance simulation and design optimisation of trilateral-cycle engines for waste heat recovery-to-power generation. Applied Energy. Elsevier Ltd; 2015; 154: 26–34. Available at: DOI:10.1016/j.apenergy.2015.04.095
16. Dong TMH., Nguyen XP. Exhaust gas recovery from marine diesel engine in order to reduce the toxic emission and save energy: A mini review. Journal of Mechanical Engineering Research and Developments. 2019; 42(5): 143–147. Available at: DOI:10.26480/jmerd.05.2019.143.147
17. Brighenti GD. Performance and assessment of s-CO2 bottoming cycles for GT-based power plants for commercial marine applications. Cranfield University; 2014.
18. Fang L., Li Y., Yang X., Yang Z. Analyses of Thermal Performance of Solar Power Tower Station Based on a Supercritical CO2 Brayton Cycle. Journal of Energy Resources Technology. 2020; 142(3): 1–7. Available at: DOI:10.1115/1.4045083
19. Carlson M., Alvarez F. DESIGN OF A 1 MWTH SUPERCRITICAL CARBON DIOXIDE PRIMARY HEAT EXCHANGER TEST SYSTEM. Journal of Energy Resources Technology. December 2020; : 1–34. Available at: DOI:10.1115/1.4049289
20. Marchionni M., Bianchi G., Tassou SA. Review of supercritical carbon dioxide (sCO2) technologies for high-grade waste heat to power conversion. SN Applied Sciences. Springer International Publishing; 2020; 2(4): 1–13. Available at: DOI:10.1007/s42452-020-2116-6
21. Vesely L., Manikantachari KRV., Vasu S., Kapat J., Dostal V., Martin S. Effect of impurities on compressor and cooler in supercritical CO2 cycles. Journal of Energy Resources Technology, Transactions of the ASME. 2019; 141(1): 1–8. Available at: DOI:10.1115/1.4040581
22. Hou S., Zhang W., Zeng Z., Ji J. Supercritical CO2 Cycle System Optimization of Marine Diesel Engine Waste Heat Recovery. 2015; : 178–183. Available at: DOI:10.2991/aeece-15.2015.36
23. Sharma OP., Kaushik SC., Manjunath K. Thermodynamic analysis and optimization of a supercritical CO2 regenerative recompression Brayton cycle coupled with a marine gas turbine for shipboard waste heat recovery. Thermal Science and Engineering Progress. 2017; 3: 62–74. Available at: DOI:10.1016/j.tsep.2017.06.004
24. Di Bella FA. Gas Turbine Engine Exhaust Waste Heat Recovery Using Supercritical CO2 Brayton Cycle With Thermoelectric Generator Technology. ASME 2015 9th International Conference on Energy Sustainability collocated with the ASME 2015

Power Conference, the ASME 2015 13th International Conference on Fuel Cell Science, Engineering and Technology, and the ASME 2015 Nuclear Forum. ASME Digital Collection; 2015. Available at: DOI:10.1115/ES2015-49059

25. Islam S., Dincer I. A comparative study of syngas production from two types of biomass feedstocks with waste heat recovery. Journal of Energy Resources Technology, Transactions of the ASME. 2018; 140(9): 1–11. Available at: DOI:10.1115/1.4039873
26. Ogidiama OV., Abu Zahra M., Shamim T. Techno-Economic Analysis of a Carbon Capture Chemical Looping Combustion Power Plant. Journal of Energy Resources Technology. 2018; 140(11): 1–11. Available at: DOI:10.1115/1.4040193
27. Aspen Plus V11. PENG-ROB. Aspen Technology; 2019.
28. Yang MH. Optimizations of the waste heat recovery system for a large marine diesel engine based on transcritical Rankine cycle. Energy. Elsevier Ltd; 2016; 113: 1109–1124. Available at: DOI:10.1016/j.energy.2016.07.152
29. Cha JE., Ahn Y., Seo H., Chung HJ. Development of Supercritical CO2 Power System for Waste Heat Application. Transactions of the Korean Nuclear Society Autumn Meeting. Gyeongju, Korea; 2017.
30. Cengel YA., Boles MA. Thermodynamics An Engineering Approach. 7th edn. McGraw-Hill; 2008.
31. Chowdhury JI., Asfand F., Hu Y., Balta-ozkan N., Varga L., Patchigolla K. Waste heat recovery potential from industrial bakery ovens using thermodynamic power cycles. Proceedings of ECOS 2019 - the 32nd international conference on Efficiency, cost, optimization, simulation and environmental impact of energy systems. Wroclaw, Poland: ECOS; 2019.
32. Palchak D., Suryanarayanan S., Zimmerle D. An Artificial Neural Network in Short-Term Electrical Load Forecasting of a University Campus: A Case Study. Journal of Energy Resources Technology. 2013; 135(3). Available at: DOI:10.1115/1.4023741
33. Márquez-Nolasco A., Conde-Gutiérrez RA., Hernández JA., Huicochea A., Siqueiros J., Pérez OR. Optimization and Estimation of the Thermal Energy of an Absorber With Graphite Disks by Using Direct and Inverse Neural Network. Journal of Energy Resources Technology, Transactions of the ASME. 2018; 140(2): 1–13. Available at: DOI:10.1115/1.4036544
34. Kang PS., Lim JS., Huh C. Temperature Dependence of the Shear-Thinning Behavior o Partially Hydrolyzed Polyacrylamide Solution for Enhanced Oil Recovery. Journal of Energy Resources Technology, Transactions of the ASME. 2021; 143(6): 1–9. Available at: DOI:10.1115/1.4048592
35. Wärtsilä. Wärtsilä-18V50DF. 2020. Available at: https://www.wartsila.com/marine/build/engines-and-generating-sets/dual-fuel-engines/wartsila-50df (Accessed: 14 October 2020)
36. Sung T., Kim KC. Thermodynamic analysis of a novel dual-loop organic Rankine cycle

for engine waste heat and LNG cold. Applied Thermal Engineering. 2016; 100: 1031–1041. Available at: DOI:10.1016/j.applthermaleng.2016.02.102

37. Chowdhury JI., Hu Y., Haltas I., Balta-Ozkan N., Matthew GJ., Varga L. Reducing industrial energy demand in the UK: A review of energy efficiency technologies and energy saving potential in selected sectors. Renewable & Sustainable Energy Reviews. 2018; 94: 1153–1178. Available at: DOI:10.1016/j.rser.2018.06.040
38. Persichilli M., Kacludis A., Zdankiewicz E., Held T. Supercritical CO2 Power Cycle Developments and Commercialization: Why sCO2 can Displace Steam Ste am. Power-Gen India & Central Asia 2012. New Delhi, India; 2012. pp. 19–21.
39. Bontempo R., Manna M. Work and efficiency optimization of advanced gas turbine cycles. Energy Conversion and Management. Elsevier; 2019; 195(June): 1255–1279. Available at: DOI:10.1016/j.enconman.2019.03.087
40. Ciric AR., Floudas CA. Heat exchanger network synthesis without decomposition. Computers and Chemical Engineering. 1991; 15(6): 385–396. Available at: DOI:10.1016/0098-1354(91)87017-4

Figure Captions List

Fig. 1 Schematic and T-s diagram of the Basic Brayton cycle

Fig. 2 Schematic and T-s diagram of the Recuperated cycle

Fig. 3 Schematic and T-s diagram of the Reheated cycle

Fig. 4 Validation of current model with respect to variation of optimised net work output with maximum pressure

Fig. 5 Determination of optimised mass flow rate of CO_2 for basic Brayton cycle from the waste heat data of diesel engine

Fig. 6 Summary of input parameters for sensitivity analysis

Fig. 7 Effect of variation of waste heat inlet temperature for (a) optimised net work and (b) corresponding thermal efficiency

Fig. 8 Effect of variation of waste heat inlet temperature for (a) optimised thermal efficiency and (b) corresponding net work

Fig. 9 Effect of variation of maximum pressure for (a) optimised net work and (b) corresponding thermal efficiency

Fig. 10 Effect of variation of maximum pressure for (a) optimised thermal efficiency and (b) corresponding net work

Fig. 11 Engine (Wärtsilä-18V50DF) efficiency improvement with WHR for base-case simulation

Table Captions List

Table 1 Input parameters for validation

Table 2 Base-case parameters for marine diesel engine

Table 3 Base-case results for marine diesel engine

https://dspace.org/

Design optimization of supercritical carbon dioxide (s-CO2) cycles for waste heat recovery from marine engines

Hossain, Md. J.; Chowdhury, Jahedul Islam; Balta-Ozkan, Nazmiye; Asfand, Faisal; Saadon, Syamimi ...

2021-01-29
American Society of Mechanical Engineers (ASME)
https://doi.org/10.1115/1.4050006
Hossain MJ, Chowdhury JI, Balta-Ozkan N, et al., (2021) Design optimization of supercritical carbon dioxide (s-CO2) cycles for waste heat recovery from marine engines. Journal of Energy Resources Technology, Volume 143, Issue 12, December 2021, Article number 120901

Downloaded from a DSpace repository. https://dspace.org/